Relative Orientations of the Electric Field Gradient and Susceptibility Tensors in Monoclinic Symmetry*

W. T. Oosterhuis
Department of Physics, Carnegie-Mellon University, Pittsburgh, Pennsylvania 15213
(Received 20 August 1970)

Using crystalline fields with local monoclinic symmetry and the spin-orbit interaction acting on those paramagnetic ions whose orbital state may be described by a linear combination of d_ϵ (or T_{2g}) orbitals, it is shown that the electric field gradient (EFG) and susceptibility (χ) tensors have only one common axis for their respective principal-axis systems. Expressions for the EFG and the magnetic hyperfine interactions referred to the magnetic axes are presented to include the effects of monoclinic symmetry. The reorientation of the magnetic and EFG principal axes may have marked effects on the Mössbauer and NMR spectra where the nuclear probe is sensitive to both magnetic and electric hyperfine interactions. Some examples are presented and Mössbauer spectra calculated to show the effects of monoclinic symmetry.

I. INTRODUCTION

Recently the orientations of the electric field gradient (EFG) and susceptibility ($\tilde{\chi}$) tensors have been determined in several iron salts.[1-3] It is interesting to note that in those crystals where there is monoclinic symmetry at the iron site, the principal-axis system (PAS) of the EFG tensor and the PAS of the susceptibility tensor are not the same although the local monoclinic (twofold) axis is a common axis. In some cases the EFG and susceptibility measurements were made on the same crystal sample. These workers have interpreted their results in terms of an orthorhombic crystal field and have explained the nonalignment of the principal axis systems of the EFG and $\tilde{\chi}$ as being due to the monoclinic symmetry.

It was shown in an earlier work,[3] that when a monoclinic crystal field is used, and the electron ground state was a single electron or hole ($S=\frac{1}{2}$), then nonalignment of the EFG and $\tilde{\chi}$ is expected. However, this fact may have been obscured in the particular example to which the calculation was applied [$K_3Fe(CN)_6$] in which the x axis of the EFG became colinear with the y axis of the $\tilde{\chi}$-tensor PAS. Thus the distinction between the relative orientations of the EFG and $\tilde{\chi}$ PAS tended to be disguised in this compound.

This distinction between the orientation of the EFG and magnetic PAS becomes important in fitting experimental Mössbauer spectra, because the nuclear levels can be mixed in such a way that normally forbidden transitions may appear in the spectrum as well as shifts in the energies of some transitions and changes in their intensities.

It is our purpose to show for the electronic system with a single electron in a d_ϵ orbital external to a filled subshell that the EFG and $\tilde{\chi}$ tensors will become reoriented with respect to each other under monoclinic symmetry. There are many electronic configurations that would behave in a similar manner because they can also be discussed in terms of a single d_ϵ orbital state. Examples of these configurations are found in nature as shown in Table I.

We will use a simple crystal field model and not worry about the relative strengths of the ligand fields or covalency, since it is the symmetry which is important to obtain the results with which we are concerned. We also will operate with this crystal field on a high-spin ferrous ion as our example, although similar specific calculations will show the same results for the other electronic configurations where the orbital state is represented by a linear combination of the d_ϵ states such as the low-spin ferric case.[3]

II. ELECTRONIC STATE

The high-spin Fe^{++} ion has a $^5D_4$ ground state where there are six electrons obeying Hund's rule in which five of the electrons occupy the five different $3d$ orbitals with parallel spins and the sixth electron enters one of these $3d$ orbits with its spin opposed to the other five. This gives four unpaired electron spins ($\tilde{S}=2$) and the orbital part of the problem may be treated as a single electron external to a spherical shell of charge.

TABLE I. Electronic configurations found in nature for various monoclinic salts.

Salt	Electronic config.	Angle between χ and EFG	Ref.
$FeCl_2\cdot 4H_2O$	$d_\epsilon^4 d_\gamma^2$	25°	1
$Fe(SO_4NH_4)_2\cdot 6H_2O$	$d_\epsilon^4 d_\gamma^2$	72° (18°)	2
$K_3Fe(CN)_6$	d_ϵ^5	90°	3
$K_4Mn(CN)_6$	d_ϵ^5	26° [a]	4
MyN_3	d_ϵ^5	29° [a]	5

[a]These are the measured angles between the octahedral axes and the g-tensor axes.

The large crystal field of cubic symmetry due to the octahedral coordination demands that the sixth electron be one of, or a linear combination of, the d_ϵ orbital states. Because the cubic crystal field splitting is so great in comparison to kT and the spin-orbit and rhombic interactions, it is usually a good approximation to treat the d_ϵ orbitals as isolated.

The threefold orbital degeneracy is lifted by placing the complex ion in a noncubic environment or by a Jahn-Teller distortion. We will treat this as a crystal field acting on the orbitals and solve the problem of a crystal field combined with spin-orbit interactions.

Relative to the cubic axes (which might join the ligands to the Fe) the d_ϵ basis states are defined as follows:

$$\begin{aligned} |x'y'\rangle &= i(Y'^{2}_{2} - Y'^{-2}_{2})/\sqrt{2}\,, \\ |x'z'\rangle &= -(Y'^{1}_{2} - Y'^{-1}_{2})/\sqrt{2}\,, \\ |y'z'\rangle &= i(Y'^{1}_{2} + Y'^{-1}_{2})/\sqrt{2}\,, \end{aligned} \tag{1}$$

where $x'y'z'$ are the cubic axes of the complex molecule and the Y^m_2 are the spherical harmonics, the prime on these spherical harmonics refers them to the cubic axes. Suppose now that the system experiences a distortion of low symmetry which may be represented as a crystal field potential ($V_{\rm rh}$) with rhombic symmetry.

$V_{\rm rh} = (A\bar{z}^2 + B\bar{x}^2 + C\bar{y}^2)$, where $A+B+C=0$ as required by Laplace's equation and $\bar{x}\,\bar{y}\,\bar{z}$ are the principal axes of $V_{\rm rh}$. If the primed and barred axis systems are identical, then the wave functions (1) are energy eigenstates in the orthorhombic crystal field. However, imagine that the $V_{\rm rh}$ field is rotated by an angle γ about the z' axis, the cubic field (x', y', z') remaining fixed, so that the total crystal field has monoclinic symmetry with one common (twofold) axis, the $z'=z$ axis (see Fig. 1). So we have the transformation

$$\begin{aligned} \bar{x} &= x'\cos\gamma + y'\sin\gamma\,, \\ \bar{y} &= -x'\sin\gamma + y'\cos\gamma\,, \\ \bar{z} &= z'\,, \end{aligned} \tag{2}$$

and the crystal field Hamiltonian with monoclinic symmetry is

$$\begin{aligned} H &= D(x'^4 + y'^4 + z'^4 - \tfrac{3}{5}r^4) + (A\bar{z}^2 + B\bar{x}^2 + C\bar{y}^2) \\ &= V_{\rm cubic} + [Az'^2 + (B\sin^2\gamma + C\cos^2\gamma)y'^2 \\ &\quad + (B\cos^2\gamma + C\sin^2\gamma)x'^2 + (B-C)\sin 2\gamma\, x'y']\,. \end{aligned} \tag{3}$$

Diagonalization of the Hamiltonian matrix within the basis set defined relative to the cubic axes (1) gives three eigenstates which may be written as

$$|a\rangle = l_{zz}|x'y'\rangle + l_{zy}|x'z'\rangle + l_{zx}|y'z'\rangle\,,$$

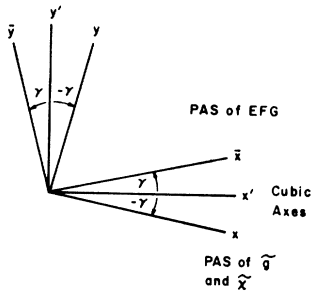

FIG. 1. Diagram showing the orientations of the three axis systems. ($x'y'z'$) are the axes of the cubic potential; ($\bar{x}\,\bar{y}\,\bar{z}$) are the principal axes of the rhombic potential and the electric field gradient; (xyz) are the principal axes of the g and χ tensors.

$$\begin{aligned} |b\rangle &= l_{xz}|x'y'\rangle + l_{xy}|x'z'\rangle + l_{xx}|y'z'\rangle\,, \\ |c\rangle &= l_{yz}|x'y'\rangle + l_{yy}|x'z'\rangle + l_{yx}|y'z'\rangle\,, \end{aligned} \tag{4}$$

where

$$\begin{aligned} &l_{zz}=1\,, && l_{xz}=l_{zx}=l_{yz}=l_{zy}=0\,, \\ &l_{xx}=l_{yy}=\cos\gamma\,, && l_{yx}=-l_{xy}=\sin\gamma\,. \end{aligned} \tag{5}$$

Now the states $|a\rangle$, $|b\rangle$, and $|c\rangle$ are energy eigenstates of the monoclinic crystal field. The contours of $|b\rangle$ and $|c\rangle$ rotate with the rotating rhombic field, but the state $|a\rangle$ remains as $|x'y'\rangle$ aligned in the cubic axis system. The expressions (4) represent a rotation in *function* space. Since these eigenstates are orthonormal, the coefficients l_{ij} behave like a set of direction cosines relating one set of axes to another.

A. Magnetic Axes

Next let us define a third axis system (xyz) which is related to the cubic axes ($x'y'z'$) by these "direction cosines" (Fig. 1.),

$$x_i = l_{ij}x'_j\,. \tag{6}$$

Note that the xyz system is a system which rotates about z' through an angle $-\gamma$. Bleaney and O'Brien[4] have shown that the problem is simplified if the angular momentum operators are expressed in the unprimed axis system. Since $\vec{L}$ is a vector, $L_i = l_{ij}L'_j$. Following Bleaney and O'Brien the nonzero matrix elements of $\vec{L}$ are

$$\begin{aligned} \langle x'y'|L_{y'}|y'z'\rangle &= \langle y'z'|L_{z'}|x'z'\rangle \\ &= \langle x'z'|L_{x'}|x'y'\rangle = +ik\,, \\ \langle y'z'|L_{y'}|x'y'\rangle &= \langle x'z'|L_{z'}|y'z'\rangle \\ &= \langle x'y'|L_{x'}|x'z'\rangle = -ik\,, \end{aligned}$$

where the orbital reduction factor k allows for pos-

sible covalency effects. Thus

$$\langle a|L_i|b\rangle = -\langle b|L_i|a\rangle = ikl_{ij}l_{yj} = ik\delta_{iy}\,,$$
$$\langle b|L_i|c\rangle = -\langle c|L_i|b\rangle = ikl_{ij}l_{zj} = ik\delta_{ix}\,, \qquad (7)$$
$$\langle c|L_i|a\rangle = -\langle a|L_i|c\rangle = ikl_{ij}l_{xj} = ik\delta_{iz}\,.$$

So the (xyz) are the PAS for the orbital angular momentum operators. One can then introduce the spin variable quantized in the (xyz) system and the basis states are written as $|a, m\rangle$, where $m = \pm 2$, ± 1, 0 for the Fe^{++} ion. The spin-orbit interaction will mix these states and remove some of the degeneracies.

Diagonalization of the Hamiltonian $\mathcal{H}_0 = (A\bar{z}^2 + B\bar{x}^2 + C\bar{y}^2) + \lambda\vec{L}\cdot\vec{S}$ will yield eigenstates of the form $|n\rangle = \sum_m\{a_{nm}|a, m\rangle + b_{nm}|b, m\rangle + ic_{nm}|c, m\rangle\}$, where $m = S_z$ and the energy of the state is E_n.[6]

The magnetic susceptibility as a second-rank tensor may be expressed in terms of its components χ_{ij}, where $i = x$, y, or z. These quantities χ_{ij} may be calculated by using the energies E_n and wave functions $|n\rangle$. In paramagnetic materials the magnetic energy $\beta_e\vec{\mathbf{H}}_{ap}\cdot(\vec{L} + 2\vec{S}) = \beta_e\vec{\mathbf{H}}_{ap}\cdot\vec{P}$ is much smaller than the other terms (H_{ap} is the applied magnetic field). The magnetization $\vec{M}$ is given by

$$\vec{M} = \sum_n\langle n|\beta_e\vec{P}|n\rangle e^{-\beta E_n}/\sum_n e^{-\beta E_n}, \quad \beta = 1/kT\,.$$

Making the assumption that $|\vec{\mathbf{H}}_{ap}|$ is small it can be shown that the susceptibility χ_{ij} may be expressed as

$$\chi_{ij} = \frac{\partial M_i}{\partial H_j} = \beta_e^2\sum_n\left\{\frac{\langle n|P_i|n\rangle\langle n|P_j|n\rangle}{kT}e^{-\beta E_n} + \sum_q\frac{\langle n|P_i|q\rangle\langle q|P_j|n\rangle}{E_q - E_n}(e^{-\beta E_q} - e^{-\beta E_n})\right\}\Big/\sum_n e^{-\beta E_n}\,.$$

The matrices P_x, P_y, P_z may be calculated in the basis set $|a, m\rangle$, $|b, m\rangle$, and $i|c, m\rangle$, where $m = S_z$. In the case of the Fe^{2+} ion, these matrices are 15×15 arrays. One can calculate the matrix elements $\langle n|P_i|m\rangle$, where the states $|n\rangle$ are determined from the Hamiltonian $\mathcal{H}_0$. These calculations are facilitated by the use of a computer and it is found that $\langle n|P_i|m\rangle\langle m|P_j|n\rangle \simeq 0$ for all $|n\rangle$ and $|m\rangle$, where $i \neq j$ as long as the applied field $\vec{\mathbf{H}}_{ap}$ is small. Thus the (xyz) system is the magnetic PAS for small applied fields.

In the system $(\bar{x}\bar{y}\bar{z})$ rotated about the z axis through an angle $+2\gamma$ relative to the (xyz) axes we have

$$\chi_{\bar{x}\bar{x}} = \chi_{xx}\cos^2 2\gamma + \chi_{yy}\sin^2 2\gamma\,,$$
$$\chi_{\bar{y}\bar{y}} = \chi_{xx}\sin^2 2\gamma + \chi_{yy}\cos^2 2\gamma\,,$$
$$\chi_{\bar{z}\bar{z}} = \chi_{zz}\,,$$
$$\chi_{\bar{x}\bar{y}} = \tfrac{1}{2}(\chi_{yy} - \chi_{xx})\sin 4\gamma\,.$$

So in the $(\bar{x}\bar{y}\bar{z})$ system, which is the PAS of the rhombic crystal field, it is found that $\chi_{\bar{x}\bar{y}} \neq 0$ if $\chi_{xx} \neq \chi_{yy}$ and if $\gamma \neq 0$.

When the applied field becomes larger, the χ tensor begins to have nonzero off-diagonal terms (in the xyz system). This indicates that the tensor is rotating or that excited states are being admixed to the ground state. A similar effect has been discussed by Jordahl[7] in that when the excited states have different thermal populations the χ tensor will have different orientations.

B. Calculation of the EFG

The electric-field-gradient tensor will follow the rotation of the rhombic field as one expects intuitively, since the EFG does not "see" the cubic potential. As mentioned previously a rotation of the rhombic field about the z' axis will move the contours of the states $|b\rangle$ and $|c\rangle$, but leave $|a\rangle$ unchanged. Thus if $\gamma \neq 0$, the d_ϵ states look like $|\bar{x}\bar{z}\rangle$, $|\bar{y}\bar{z}\rangle$, and $|x'y'\rangle$. One can also see that the states $|b\rangle$ and $|c\rangle$ do not rotate if $B = C$ in the rhombic potential expressed in (3).

The quadrupole interaction may be written as

$$H_Q = \frac{eQ}{4I(2I-1)}\{V_{zz}[3I_z^2 - I(I+1)] + V_1(I_-I_z + I_zI_-) + V_{-1}(I_+I_z + I_zI_+) + V_{-2}I_+^2 + V_2I_-^2\}, \qquad (8)$$
$$V_{zz} = Y_2^0(16\pi/5)^{1/2}\langle r^{-3}\rangle,$$

where

$$V_{\pm 1} = V_{xz} \pm iV_{yz} = \mp(24\pi/5)^{1/2}\,Y_2^{\pm 1}\,\langle r^{-3}\rangle,$$
$$V_{\pm 2} = \tfrac{1}{2}\{V_{xx} - V_{yy} \pm 2iV_{xy}\} = -(24\pi/5)^{1/2}\,Y_2^{\pm 2}\,\langle r^{-3}\rangle.$$

So we need the matrix elements of the operators Y_2^l. These operators can be expressed in the different axis systems with the following relations:

$$Y_2^0 = Y_2'^0 = \overline{Y}_2^0,$$
$$Y_2^{\pm 1} = Y_2'^{\pm 1}\,e^{\pm i\gamma} = \overline{Y}_2^{\pm 1}e^{\pm 2i\gamma},$$
$$Y_2^{\pm 2} = Y_2'^{\pm 2}\,e^{\pm 2i\gamma} = \overline{Y}_2^{\pm 2}e^{\pm 4i\gamma}.$$

Calculations of the matrix elements of these operators $\langle n|Y_2^l|n\rangle$ yield the following expressions in the (xyz) system for $S_z = m$ (c.c. means the complex conjugate of the term immediately preceding):

$$\langle n|V_{zz}|n\rangle = \sum_m\{+\tfrac{4}{7}|a_{nm}|^2 - \tfrac{2}{7}(|b_{nm}|^2 + |c_{nm}|^2)\}\langle r^{-3}\rangle, \qquad (9a)$$

$$\langle n|V_{\pm 1}|n\rangle = \sum_m -\tfrac{3}{7}\{(a_{nm}^*b_{nm} \pm a_{nm}c_{nm}^*) + \text{c. c.}\}\langle r^{-3}\rangle\,, \qquad (9b)$$

$$\langle n|V_{\pm 2}|n\rangle = \sum_m\tfrac{3}{7}(|b_{nm}|^2 - |c_{nm}|^2)\,e^{\pm 4i\gamma}\langle r^{-3}\rangle$$

$$= \langle n | \tfrac{1}{2}(V_{xx} - V_{yy}) \pm iV_{xy} | n \rangle . \qquad (9c)$$

In the PAS of the EFG, $V_{\bar{x}\bar{y}} = V_{\bar{y}\bar{z}} = V_{\bar{x}\bar{z}} = 0$. However, in the axis system (xyz) rotated by $(-\gamma)$ about the common z axis, one finds that $V_{xy} \neq V_{yz} = V_{xz} = 0$. $V_{xz} = V_{yz} = 0$ because $\langle a, m | Y_2^{\pm 1} | b, m \rangle$ and $\langle a, m | Y_2^{\pm 1} | c, m \rangle$ are the only nonzero matrix elements to be found for this operator. However, the spin states must be the same and eigenstates found in small applied fields give *either* (a_{nm}) *or* $(b_{nm}$ and $c_{nm})$ as zero for a given spin state m. When the applied field becomes large (say several kilogauss) then these $V_{\pm 1}$ matrix elements are no longer negligible. For the moment however, we will concentrate on the small-field case in which the EFG's and χ's were actually measured. Thus

$$\langle n | V_{xx} - V_{yy} | n \rangle = \sum_m \tfrac{6}{7} (|b_{nm}|^2 - |c_{nm}|^2) \langle r^{-3} \rangle \cos 4\gamma$$

and

$$\langle n | V_{xy} | n \rangle = \sum_m \tfrac{3}{7} (|b_{nm}|^2 - |c_{nm}|^2) \langle r^{-3} \rangle \sin 4\gamma .$$

One can also see by comparing terms that

$$\langle n | V_{\pm 2} | n \rangle = \sum_m \tfrac{3}{7} (|b_{nm}|^2 - |c_{nm}|^2) e^{\pm 4i\gamma} \langle r^{-3} \rangle$$

$$= \langle n | \tilde{V}_{\pm 2} e^{\pm 4i\gamma} | n \rangle ,$$

$$\langle n | V_{\bar{x}\bar{x}} - V_{\bar{y}\bar{y}} | n \rangle = \sum_m \tfrac{6}{7} (|b_{nm}|^2 - |c_{nm}|^2) \langle r^{-3} \rangle ,$$

$$\langle n | V_{\bar{x}\bar{y}} | n \rangle = 0 .$$

Therefore $V_{\bar{x}\bar{y}} = 0$ (as do $V_{\bar{x}\bar{z}}$ and $V_{\bar{y}\bar{z}}$) so that the $(\bar{x}\bar{y}\bar{z})$ is the PAS for the EFG and this result is independent of the spin. Thus, for the EFG expressed in the xyz system of axes, $\eta q = V_{xx} - V_{yy} \pm 2iV_{xy}$ must contain a factor $e^{4i\gamma}$. One finds it easier to do nuclear energy-level calculations in the (xyz) system when magnetic interactions exist, and to include the factors $e^{4i\gamma}$ in the expressions for nq.[8]

The total EFG seen by the nucleus is the Boltzmann average over all states $|n\rangle$ weighted with the factors $e^{-\beta E_n}$ $(\beta = 1/kT)$,

$$q = \sum_n \sum_m \{ + \tfrac{4}{7} |a_{mn}|^2 - \tfrac{2}{7} (|b_{mn}|^2 + |c_{mn}|^2) \} \times e^{-\beta E_n} \langle r^{-3} \rangle / \sum_n e^{-\beta E_n} , \qquad (10a)$$

$$nq = \sum_n \sum_m \{ \tfrac{6}{7} (|b_{mn}|^2 - |c_{mn}|^2) \times e^{-\beta E_n} e^{\pm 4i\gamma} \langle r^{-3} \rangle \} / \sum_n e^{-\beta E_n} \qquad (10b)$$

[expressed in the (xyz) system].

When the applied magnetic field becomes large then one begins to obtain small, but nonzero matrix elements for $\langle n | V_{\pm 1} | n \rangle$. Thus the (xyz) system may not be the PAS for the EFG when a field of several kG is applied. This is similar to the effect on the χ tensor when the applied field becomes large enough to admix some of the excited states.

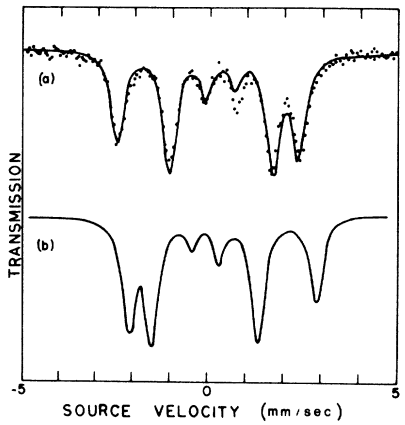

FIG. 2. Mössbauer spectrum of single-crystal $K_3Fe(CN)_6$. Applied field is 29 kG along the a' axis of the crystal and the radiation is along the c axis at 4.2 °K. The solid curves are calculations with $A = 0.093\lambda$, $B = 0.322\lambda$, $\lambda = -278\,\mathrm{cm}^{-1}$ and (a) $\gamma = 45°$ (monoclinic symmetry); (b) $\gamma = 0°$ (orthorhombic symmetry).

C. Magnetic Hyperfine Interaction

The magnetic hyperfine interaction is also affected by monoclinic symmetry in the crystalline electric field. The well-known interaction is

$$\mathcal{H}_M = 2g_n\beta_e\beta_n \langle r^{-3} \rangle \{ \vec{I} \cdot \vec{L} + 3(\vec{I} \cdot \hat{r}) \vec{S} \cdot \hat{r} - \vec{I} \cdot \vec{S} - \kappa \vec{I} \cdot \vec{S} \} . \qquad (11)$$

For spin-$\frac{1}{2}$ iron salts, this interaction may be written as[3]

$$\mathcal{H}_M = \vec{I} \cdot \vec{A} \cdot \vec{S}_{\mathrm{eff}} \text{ with } |+\rangle = a|a, \alpha\rangle + b|b, \beta\rangle + ic|c, \beta\rangle$$

for one member of the ground-state Kramer's doublet:

$$A_x + A_y + 2iC_{xy} = P\{4a(b+c) - 2(\kappa - \tfrac{2}{7})a^2 - \tfrac{6}{7}[a(b+c) - (b-c)^2 e^{4i\gamma}]\} ,$$

$$A_x - A_y = P\{4a(c-b) - 2(\kappa + \tfrac{1}{7})(c^2 - b^2) + \tfrac{6}{7}a(c-b)\} ,$$

$$A_z = P\{-4bc - (1+\kappa)(a^2 - b^2 - c^2) + \tfrac{3}{7}(a^2 - 3b^2 - 3c^2) + \tfrac{6}{7}a(b+c)\} ,$$

where γ is the same angle which denotes the rotation of the rhombic field from the cubic axes.

In the example of $K_3Fe(CN)_6$ the effect of a nonzero γ upon the Mössbauer spectrum can be seen in Fig. 2. This effect appears in both single-crystal *and* powder experiments. The solid curves are calculated using the expressions for the $\vec{A}$ and EFG tensors (given above) and the electronic states $|+\rangle$ and $|-\rangle$ as determined by the rhombic field

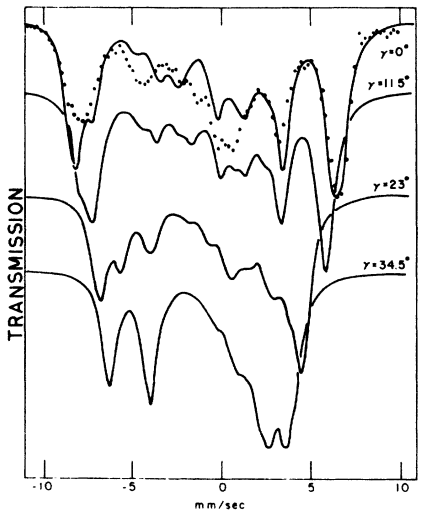

FIG. 3. Mössbauer spectra of $Na_2Fe(CN)_5NH_3$ diluted in DMF at 4.2 °K in zero applied field. The solid curves are calculated using $A = 0.296\lambda$, $B = 1.328\lambda$, $\lambda = -300\ cm^{-1}$, and (a) $\gamma = 0°$; (b) $\gamma = 11.5°$; (c) $\gamma = 23°$; (d) $\gamma = 34.5°$. It appears that this spin-1/2 salt has an electronic configuration which is very nearly orthorhombic in this environment.

and spin-orbit coupling.

Still another example of an $S = 1/2$ iron salt is $Na_2Fe(CN)_5NH_3$ diluted in DMF [Fig.3(a) – unpublished data]. Although the agreement between experiment and calculation is not good, it appears that deviations from orthorhombic symmetry make the situation considerably worse.

For iron salts with spin 2 (high-spin ferrous) the hyperfine interaction has been calculated with the results presented in the Appendix. These expressions differ from those of Lang and Johnson[9] as we have not used a spin Hamiltonian.

The effects of a variable γ can be seen in Fig. 4 where Mössbauer spectra have been calculated for a powder sample of $FeCl_2 \cdot 4H_2O$. Crystal field parameters $A = 17\,670\ cm^{-1}$, $B = 28\,000\ cm^{-1}$, $\lambda = -80\ cm^{-1}$ have been used to calculate the electronic state. An applied field of 1.9 kG along the y axis has been used to simulate the Weiss molecular field acting on the Fe^{+2} ion which in turn creates a hyperfine field of 266 kG at the site of the ^{57}Fe nucleus. For $FeCl_2 \cdot 4H_2O$, the angle between the Weiss field (and the hyperfine field) along the y axis of the magnetic PAS and the major axis of the field gradient ($\bar{x}$ axis) is $90-2\gamma$ (refer to Fig. 1). The best agreement with experiment is with $\gamma = 32.5°$ which is also in agreement with the results of Ono *et al.*[1]

From these results one is able to determine the angle γ within a few degrees in the Mössbauer data, even if one has a powder sample, as long as a large magnetic hyperfine interaction exists. The sign of γ makes no difference in the calculated spectrum as one expects from physical intuition.

III. DISCUSSION

We have seen that if one has an orbital state described by a d_ϵ orbital in a monoclinic crystal field, one may expect the principal-axis systems of the EFG and χ tensors to be differently oriented, but to have one common local twofold axis. In some cases the local twofold axis is perpendicular to the monoclinic axis of the crystal. Specific calculations have been carried out for the $d_\epsilon^4 d_\gamma^2$ and d_ϵ^5 configurations. These results appear to explain the experimental results in several iron salts[1-3] where the orientation of EFG has been determined by Mössbauer area ratio measurements to be different from that of the χ tensor.

The analysis in Sec. II indicates that the axes of the cubic electric field bisect the angle between the EFG and χ tensors. It is not necessarily true that the cubic axes be aligned with ligand axes as there are several cases where the ligand axes are not orthogonal.

It is interesting to note that as the rhombic field rotates away from the cubic axes through an angle γ, the EFG follows the rhombic field, but the χ

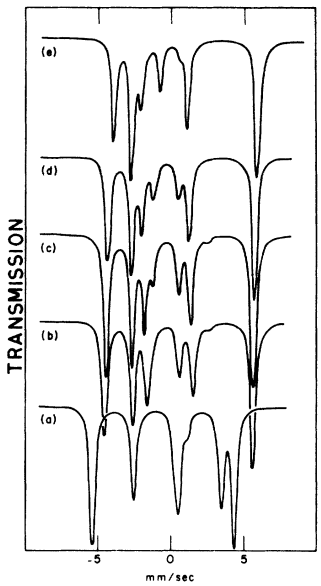

FIG. 4. Mossbauer spectra calculated for a powder sample of $FeCl_2 \cdot 4H_2O$ with $A = 17\,670\ cm^{-1}$, $B = 28\,000\ cm^{-1}$, $\lambda = -80\ cm^{-1}$, $T = 0.5$ °K and (a) $\gamma = 0°$; (b) $\gamma = 30°$; (c) $\gamma = 32.5°$; (d) $\gamma = 35°$; (e) $\gamma = 45°$. It is apparent that (c) gives the best fit in agreement with Ref. 1. This means that the EFG and magnetic axes are separated by about 25°. In order to create the magnetic hyperfine field of 266 kG, 1.9 kG was applied along the y axis at $T = 0.5$ °K. This may be interpreted as the Weiss molecular field in the antiferromagnetic $FeCl_2 \cdot 4H_2O$.

tensor PAS rotates through an angle $(-\gamma)$. This is somewhat in analogy to the case where a perturbation mass is added to a mass with cubic symmetry and the inertia tensor acquires a nonzero off-diagonal component. Then the angular momentum acquires a component directed away from the symmetry axis in the direction opposite to the perturbation mass.

Mössbauer spectra have been calculated to exhibit the effect of different degrees of monoclinic symmetry. Spectra of slowly relaxing paramagnets taken in the absence of an external field and in small applied fields are sensitive to the difference between orthorhombic and monoclinic electric fields. Thus there is significant dependence in the Mössbauer spectra upon the parameter γ for low-spin ($S=\frac{1}{2}$) configurations under the condition of long relaxation times.

One does not usually observe the effects of long relaxation times in high-spin ferrous materials (with an even number of electrons), but one can see the effects of monoclinic symmetry using values of H/T (to create a sufficiently large magnetization) in paramagnets or in materials that become magnetically ordered. However, when the external field becomes large, then off-diagonal terms are created in the EFG and χ tensors relative to the PAS determined in the limit of small applied fields.

Jordahl[7] has shown that the orientation of the magnetic PAS may change with temperature and this was verified in several cases. With this result one might also expect to observe the EFG to rotate about the local diad axis with T in a manner related to the rotation of the χ tensor. It is not known whether this behavior has been observed.

In conclusion, one may interpret either susceptibility or EFG measurements in terms of a rhombic crystal field even if the paramagnetic site is in a monoclinic environment. However, the tensors will be differently oriented in monoclinic symmetry and both measurements are needed to determine if the symmetry is less than rhombic, in the absence of x-ray data, of course.

It may be possible that the reorientation of the EFG and χ tensors will take place for configurations other than those presented here as examples. One should also expect that any experiment (NMR, for example) involving a nucleus sensitive to both electric and magnetic hyperfine interactions will be affected by the relative orientation of the EFG and χ tensors.

ACKNOWLEDGMENTS

The author would like to thank Dr. George Lang, Dr. S. Friedberg, and Dr. F. de S. Barros for helpful discussions, and Dr. R. B. Griffiths for the expression for the susceptibility tensor.

APPENDIX: THE MAGNETIC HYPERFINE FIELD

The magnetic hyperfine interaction is given by the operator $\mathcal{H}_M$, which may also be expressed as an internal magnetic field $\vec{H}_{int}$,

$$\mathcal{H}_M = P\{\vec{I}\cdot\vec{L} + 3(\vec{I}\cdot\hat{r})(\vec{S}\cdot\hat{r}) - \vec{I}\cdot\vec{S} - \kappa\vec{I}\cdot\vec{S}\} = -\beta_n g_n \vec{H}_{int}\cdot\vec{I}\,, \tag{A1}$$

where $P = 2g_n\beta_n\beta_e\langle r^{-3}\rangle$ and $\vec{H}_{int} = -2\beta_e\langle r^{-3}\rangle\{\vec{L} + 3(\vec{S}\cdot\hat{r})\hat{r} - (1+\kappa)\vec{S}\}$. If one calculates the matrix elements $\langle n|\mathcal{H}_M|n\rangle$, where

$$|n\rangle = \sum_m \{a_{nm}|a, m\rangle + b_{nm}|b, m\rangle + ic_{nm}|c, m\rangle\}, \quad m = S_z$$

then the components of the internal field are given as follows. The a_{nm}, b_{nm}, and c_{nm} are determined by diagonalization of the Hamiltonian $V_{rh} + \lambda\vec{L}\cdot\vec{S} + \beta_e\vec{H}_{ap}\cdot(\vec{L}+2\vec{S})$:

$$\langle n|(H_{int})_z|n\rangle = -2\beta_e\langle r^{-3}\rangle\sum_m\{-(b^*_{nm}c_{nm} + \text{c. c.}) - (\kappa+\tfrac{4}{7})m|a_{nm}|^2 - (\kappa-\tfrac{2}{7})m(|b_{nm}|^2 + |c_{nm}|^2) + \tfrac{3}{7}[(S-m)(S+m+1)]^{1/2}[(a^*_{nm+1}b_{nm} + a^*_{nm+1}c_{nm} + a_{nm}b^*_{nm+1} - a_{nm}c^*_{nm+1}) + \text{c. c.}]\}\,, \tag{A2}$$

$$\langle n|(H_{int})_x|n\rangle = -2\beta_e\langle r^{-3}\rangle\sum_m\{(a_{nm}c^*_{nm} + \text{c. c.}) - (\kappa-\tfrac{2}{7})[(S-m)(S+m+1)]^{1/2}\tfrac{1}{2}(a^*_{nm+1}a_{nm} + \text{c. c.}) - (\kappa+\tfrac{1}{7})[(S-m)(S+m+1)]^{1/2}\tfrac{1}{2}[(b^*_{nm+1}b_{nm} + c^*_{nm+1}c_{nm}] + \text{c. c.}) + \tfrac{6}{7}m\tfrac{1}{2}(a^*_{nm}b_{nm} + \text{c. c.}) + \tfrac{3}{7}[(S-m)(S+m+1)]^{1/2}\tfrac{1}{2}[(b^*_{nm+1}c_{nm}e^{-4i\gamma} + \text{c.c.}) - (b_{nm}c^*_{nm+1}e^{4i\gamma} + \text{c. c.})]\}\,, \tag{A3}$$

$$\langle n|H_{int})_y|n\rangle = -i2\beta_e\langle r^{-3}\rangle\sum_m\{(a_{nm}b^*_{nm} - \text{c. c.}) - (\kappa-\tfrac{2}{7})[(S-m)(S+m+1)]^{1/2}\tfrac{1}{2}(a^*_{nm+1}a_{nm} - \text{c. c.}) - (\kappa+\tfrac{1}{7})[(S-m)(S+m+1)]^{1/2}\tfrac{1}{2}[(b^*_{nm+1}b_{nm} + c^*_{nm+1}c_{nm}) - \text{c. c.}] + \tfrac{6}{7}m\tfrac{1}{2}(a^*_{nm}c_{nm} - \text{c. c.}) + \tfrac{3}{7}[(S-m)(S+m+1)]^{1/2}\tfrac{1}{2}[(b^*_{nm+1}c_{nm}e^{-4i\gamma} - \text{c.c.}) - (b_{nm}c^*_{nm+1}e^{4i\gamma} - \text{c. c.})]\}\,. \tag{A4}$$

Now one may calculate the Boltzmann averages of these internal fields, i.e.,

$$\langle \vec{H}_{int} \rangle_T = \sum_n \langle n | \vec{H}_{int} | n \rangle \, e^{-\beta E_n} / \sum_n e^{-\beta E_n}$$

so that the nucleus sees the effective field as the vector sum

$$\vec{H}_{eff} = \langle \vec{H}_{int} \rangle_T + \vec{H}_{applied} \, . \qquad \text{(A5)}$$

*Work supported in part by National Science Foundation and the Office of Naval Research.

[1]P. Zory, Phys. Rev. 140, A1401 (1965); J. T. Schriempf and S. A. Friedberg, *ibid.* 136, A518 (1964); C. E. Johnson and M. S. Ridout, J. Appl. Phys. 38, 1272 (1967); K. Ono, M. Shinohara, A. Ito, T. Fujita, and A. Ishigaki, *ibid.* 39, 1126 (1968).

[2]R. Ingalls, K. Ono, and L. Chandler, Phys. Rev. 172, 295 (1968).

[3]W. T. Oosterhuis and G. Lang, Phys. Rev. 178, 439 (1969).

[4]J. M. Baker, B. Bleaney, and K. D. Bowers, Proc. Phys. Soc. (London) B69, 1205 (1956); B. Bleaney and M. C. M. O'Brien, *ibid.* B69, 1216 (1956).

[5]C. A. Helcke, D. J. E. Ingram, and E. F. Slade, Proc. Roy. Soc. (London) B169, 275 (1968).

[6]The basis states are chosen to be $|a, m\rangle$, $|b, m\rangle$, and $i|c, m\rangle$ so that the matrix elements of $\mathcal{H}_0$ are real.

[7]O. M. Jordahl, Phys. Rev. 45, 87 (1934).

[8]One can easily obtain the transformation $\frac{1}{2}(V_{xx} - V_{yy}) \pm iV_{xy} = \frac{1}{2}(V_{\bar{x}\bar{x}} - V_{\bar{y}\bar{y}}) \, e^{\pm 4i\gamma}$ by calculating $V_{ij} = \delta^2 V / \delta x_i \delta x_j$, using the chain rule and the transformation between (xyz) and $(\bar{x}\bar{y}\bar{z})$, which are separated by an angle of 2γ about a common z axis.

[9]G. Lang, Quart. Rev. Biophys. 3, 1 (1970); C. E. Johnson, Proc. Phys. Soc. (London) 92, 748, (1967).

PHYSICAL REVIEW B VOLUME 3, NUMBER 2 15 JANUARY 1971

Effect of Iron Impurities on the Thermal Conductivity of Magnesium Oxide Single Crystals below Room Temperature

I. P. Morton
Physics Department, University of Southhampton, Southhampton, England

and

M. F. Lewis
General Electric Company Ltd., Central Research Laboratories, Hirst Research Centre, Wembley, Middlesex, England

(Received 20 October 1969)

The thermal conductivity between 5 and 300 °K of magnesium oxide single crystals containing different amounts of iron impurity has been measured. The iron produces a marked reduction in the thermal conductivity with a minimum at around 80 °K in the highly doped (~ 1%) samples and we attribute this effect to resonant scattering of phonons of energy ~ 105 cm^{-1} interacting with two groups of magnetic levels of the Fe^{++} ions. We have estimated the strength of the interaction from earlier spin-lattice relaxation-time measurements. Using an expression due to Callaway for the frequency dependence of the basic phonon heat current, we have then computed the effect of this interaction on the thermal conductivity. We find that we can account substantially for the observed data by using for the resonant interaction a Lorentzian line shape with a full characteristic width equal to that observed in infrared experiments (9 cm^{-1}), but cut off at nine times the width.

I. INTRODUCTION

The theory of the thermal conductivity of dielectric solids attributes the heat transport to thermal phonon wave packets.[1] Each wave packet is characterized by a frequency ω, a mean wave vector $\vec{q}$ (and polarization p, usually uniquely determined by ω and $\vec{q}$), and a relaxation time $\tau(\omega, \vec{q})$ arising from non-wave-vector conserving processes.[2] In a certain approximation, the thermal conductivity is given by the following sum of contributions from the wave packets comprising the thermal phonon field[1]:

$$K = \tfrac{1}{3} \sum_{\omega, \vec{q}} C(\omega, \vec{q}) v^2(\omega, \vec{q}) \tau(\omega, \vec{q}) \, , \qquad (1)$$

where $C(\omega, \vec{q})$ is the specific heat per unit volume and $v(\omega, \vec{q})$ is the group velocity of the thermal phonons.

The principal problem in the theory of thermal conductivity is to compute the quantity $\tau(\omega, \vec{q})$, since it is virtually impossible to invert Eq. (1) directly so as to deduce $\tau(\omega, \vec{q})$ from measurements of K. The best that one can normally hope to achieve is a demonstration that the measurements of K are consistent with a particular calculated form of $\tau(\omega, \vec{q})$. For example, the extensive measurements and complicated analysis of Berman and Brock[3] have produced a consistent explanation for the contribution of isotope scattering to the thermal resistance of LiF. Other scattering mechanisms in-